ECCOMAS Congress 2016
VII European Congress on Computational Methods in Applied Sciences and Engineering
M. Papadrakakis, V. Papadopoulos, G. Stefanou, V. Plevris (eds.)
Crete Island, Greece, 5–10 June 2016

DIRECT FEM LARGE SCALE COMPUTATION OF TURBULENT MULTIPHASE FLOW IN URBAN WATER SYSTEMS AND MARINE ENERGY

Ezhilmathi Krishnasamy[1], Johan Hoffman[1 2], and Johan Jansson[1 2]

[1]BCAM - Basque Center for Applied Mathematics
Mazarredo 14, 48009 Bilbao, Spain
e-mail: ekrishnasamy@bcamath.org

[2] Department of High Performance Computing and Visualization KTH Royal Institute of Technology
SE-10044, Stockholm, Sweden
e-mail: {jjan,jhoffman}@kth.se

Keywords: Adaptive, FEM, Turbulence, Marine Engineering.

Abstract. *High-Reynolds number turbulent incompressible multiphase flow represents a large class of engineering problems of key relevance to society. Here we describe our work on modeling two such problems:*
1. The Consorcio de Aguas Bilbao Bizkaia is constructing a new storm tank system with an automatic cleaning system, based on periodically flushing tank water out in a tunnel.
2. In the framework of the collaboration between BCAM - Basque Center for Applied Mathematics and Tecnalia R & I, the interaction of the sea flow with a semi submersible floating offshore wind platform is computationally investigated. We study the MARIN benchmark modeling breaking waves over objects in marine environments.
Both of these problems are modeled in the the Direct FEM/General Galerkin methodology for turbulent incompressible variable-density flow [1, 2] in the FEniCS software framework.

1 INTRODUCTION

The world is facing increased climate instability and extreme weather phenomena, resulting in severe floods or drought. In the 20th century, ca. 1 million people were killed and 1.4 billion people were affected by floods [3]. Floods not only kill and affect people, they also affect the eco-systems, agriculture production, infrastructure and create economical instability. According to The International Disaster Database [4], from January 1975 to June 2002, flash floods (due to heavy rain) in Europe had 5.6 % mortality rate [3]. In Spain from 1900 to 2016, flash floods killed 987 people, 1350 people were affected and caused damage of 642 million USD [4]. It is predicted that the weather instabilities are going to worsen over the coming years [5].

Bilbao is located in the north of Spain and has Oceanic/Atlantic climate; its annual precipitation is 1200-2000 mm [6]. Consorcio de Aguas Bilbao Bizkaia (BWC) is constructing a new storm tank (detention tank) system with an automatic cleaning system, based on periodically flushing the tank out in a tunnel located in the Galindo area. This would prevent rain water flowing into the river and also minimize the hydraulic load on the existing sewer infrastructure. Later this water can be treated in the wastewater treatment plant (WWTP) in Galindo to produce potable water, or for other purposes.

The excessive water from the detention tank overflows through the tunnel, where sediments and floating objects might permanently settle on the bottom of the tunnel, which will eventually give rise to a foul smell and over time will also affect the downstream flow in the tunnel. It is not feasible to send human workers to clean the tunnel. Instead BWC wants to clean the tunnel with periodic flushing using water from the detention tank.

Our research involvement in the project has been to computationally model the water-air system, and predict the velocity, pressure and flow rate in the initial part of the tunnel. Where this velocity, pressure and flow rate values will be used as a input parameter for the shallow water modelling; and also velocity at the door section will be used to design the stronger gate to open a water from the detention tank.

We are also involved in research projects in Marine Renewable Energy (MRE) which involves similar mathematical models of water-air interaction. In the framework of the collaboration between the Basque Centre for Applied Mathematics (BCAM) and Tecnalia R&I, the interaction of the sea flow with a semisubmersible floating offshore wind platform is of key importance and high complexity.

We here take an initial step in the computational modeling in the phenomena of the platform, where we test our computational methodology on the established MARIN marine engineering benchmark.

We apply the Direct FEM/General Galerkin methodology [1, 2] to the primitive equations: variable-density incompressible Navier-Stokes, in the FEniCS-HPC software framework.

2 MATHEMATICAL MODEL

We model the problem by the primitive incompressible Navier-Stokes equations with variable density ρ:

$$
\begin{aligned}
R(\hat{u}) &= \begin{cases} \rho(\partial_t u + (u \cdot \nabla)u) + \nabla p - \nu \Delta u - \rho g = 0 \\ \partial_t \rho + (u \cdot \nabla)\rho = 0 \\ \nabla \cdot u = 0 \end{cases} \\
\hat{u} &= (u, p, \rho)
\end{aligned}
$$

By using a parameter-free stabilized finite element method (FEM) we are not introducing any explicit parametrization or modeling, aside from the slip model of the boundary layer, and we thus expect the simulations to be *predictive* if the mesh is fine enough to control the computational error.

2.1 Turbulent boundary layers

In our work on high Reynolds number turbulent flow [7, 8, 9, 10, 11], we have chosen to apply a skin friction stress as wall layer model. That is, we append the Navier-Stokes equations (NSE) with the following boundary conditions:

$$
\begin{aligned}
&u \cdot n = 0, \\
&\beta u \cdot \tau_k + n^T \sigma \tau_k = 0, \quad k = 1, 2,
\end{aligned}
$$

for $(x,t) \in \Gamma_{solid} \times I$, with $n = n(x)$ an outward unit normal vector, and $\tau_k = \tau_k(x)$ orthogonal unit tangent vectors of the solid boundary Γ_{solid}. We use matrix notation with all vectors v being column vectors and the corresponding row vector is denoted v^T.

With skin friction boundary conditions, the rate of kinetic energy dissipation in cG(1)cG(1) has a contribution of the form (for constant density):

$$
\sum_{k=1}^{2} \int_0^T \int_{\Gamma_{solid}} |\beta^{1/2} \bar{U} \cdot \tau_k|^2 \, ds \, dt,
$$

from the kinetic energy which is dissipated as friction in the boundary layer. For high Re, we model $Re \to \infty$ by $\beta \to 0$, so that the dissipative effect of the boundary layer vanishes with large Re. In particular, we have found that a small β does not influence the solution [9]. For the present simulations we used the approximation $\beta = 0$, which can be expected to be a good approximation for the high Reynolds numbers expected for the present setting.

3 COMPUTATIONAL METHODOLOGY AND SOFTWARE

The mathematical framework for the simulation method is functional analysis and the concept of weak solutions to the NSE, introduced by the mathematician Jean Leray in 1934. Leray proved that there exist weak solutions (or turbulent solutions in the terminology of Leray) that satisfy NSE in variational form, that is NSE integrated against a family of test functions.

A finite element method (FEM) is based on the variational form of NSE, and one can show that, if the formulation of the method satisfies certain conditions on stability and consistency, the approximate FEM solutions converge towards a weak solution of the NSE as the finite element mesh is refined [12]. We refer to such FEM as General Galerkin (G2) methods.

The test functions in G2 are defined over the mesh, and thus the finest scales of a G2 approximation are set by the mesh size. In contrast to RANS or LES (Large eddy simulation), no averaging operator or filter is applied to NSE, and thus no Reynolds or subgrid stresses that need modeling are introduced. Dissipation of turbulent kinetic energy in under-resolved parts of the flow is provided by the numerical stabilization of G2 in the form of a weighted least squares method based on the residual of NSE. Thus, the method is purely based on the NSE mathematical model, and no other modeling assumptions are made.

In G2, the mesh is adaptively constructed based on *a posteriori* estimation of the error in chosen goal or target functionals, such as drag and lift forces for example. Using duality in

a variational framework, *a posteriori* error estimates can be derived in terms of the residual, the mesh size, and the solution of a "dual" (or "adjoint") problem [13]. We initiate the adaptive mesh refinement algorithm from a coarse mesh, fine enough to capture the geometry, but without any further assumptions on the solution (i.e., no boundary layer meshes or *ad hoc* mesh design based on expected separation and wake structures are needed).

To model the effect of unresolved turbulent boundary layers we use a simple parametrization of the wall shear stress in terms of the skin friction [14]. In particular, for the very high Re for this problem we approximate the small skin friction by zero skin friction, which corresponds to a free slip boundary condition without boundary layer resolution.

This methodology is validated for a number of standard benchmark problems in the literature [15, 16, 17, 18], and in the following sections we describe the basic elements of the G2 method, also referred to as Adaptive DNS/LES, or simply Direct Finite element Simulation (DFS).

We have used a low order finite element discretization on unstructured tetrahedral meshes, which we refer to as cG(1)cG(1), i.e., continuous piecewise linear approximations in space and time. In this project we have not applied adaptive mesh refinement, since it currently only is functioning robustly for production simulations for constant density.

3.1 Direct FEM cG(1)cG(1) for variable-density

In a cG(1)cG(1) method [12] we seek an approximate space-time solution $\hat{U} = (D, U, P)$ (with D the discrete density ρ) which is continuous piecewise linear in space and time (equivalent to the implicit Crank-Nicolson method). With I a time interval with subintervals $I_n = (t_{n-1}, t_n)$, W^n a standard spatial finite element space of continuous piecewise linear functions, and W_0^n the functions in W^n which are zero on the boundary Γ, the cG(1)cG(1) method for variable-density incompressible flow with homogeneous Dirichlet boundary conditions for the velocity takes the form: for $n = 1, ..., N$, find $(D^n, U^n, P^n) \equiv (D(t_n), U(t_n), P(t_n))$ with $D^n \in W^n$, $U^n \in V_0^n \equiv [W_0^n]^3$ and $P^n \in W^n$, such that

$$
\begin{aligned}
r(\hat{U}, \hat{v}) &= (D((U^n - U^{n-1})k_n^{-1} + (\bar{U}^n \cdot \nabla)\bar{U}^n), v) + (2\nu\epsilon(\bar{U}^n), \epsilon(v)) \\
&- (P, \nabla \cdot v) - (Dg, v) + (\nabla \cdot \bar{U}^n, q) + (D^n - D^{n-1})k_n^{-1} + (\bar{U}^n \cdot \nabla)\bar{D}^n), v) \\
&+ LS(D^n, \bar{U}^n, P^n) + SC(D^n, \bar{U}^n, P^n) = 0, \ \forall \hat{v} = (z, v, q) \in W^n \times V_0^n \times W^n
\end{aligned} \tag{1}
$$

where $\bar{U}^n = 1/2(U^n + U^{n-1})$ is piecewise constant in time over I_n and LS and SC are least-squares and shock-capturing stabilizing term described in [12].

Here we also add an experimental phase separation term of the form $(\rho_{air} - \rho)(\rho_{water} - \rho)$. The term has only limited effect for short times. We will investigate the sensitivity of the parametrization of this term in future work for long-time simulations.

3.2 The FEniCS-HPC finite element computational framework

The simulations in this paper have been computed using the Unicorn solver in the FEniCS-HPC automated FEM software framework.

FEniCS-HPC is an open source framework for automated solution of PDE on massively parallel architectures, providing automated evaluation of variational forms given a high-level description in mathematical notation, duality-based adaptive error control, implicit parameter-free turbulence modeling by use of stabilized FEM and strong linear scaling up to thousands of cores [19, 20, 21, 22, 23, 24]. FEniCS-HPC is a branch of the FEniCS [25, 26] framework focusing on high performance on massively parallel computer architectures.

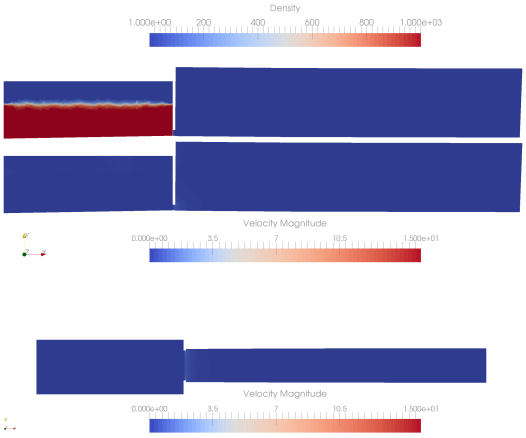

(a) Density and velocity x-y and x-z slice T_D={5s,10s}, H=6m, t=0.

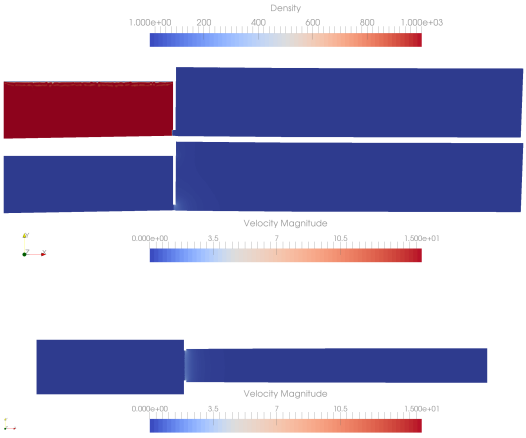

(d) Density and velocity x-y and x-z slice T_D={5s,10s}, H=10m, t=0.

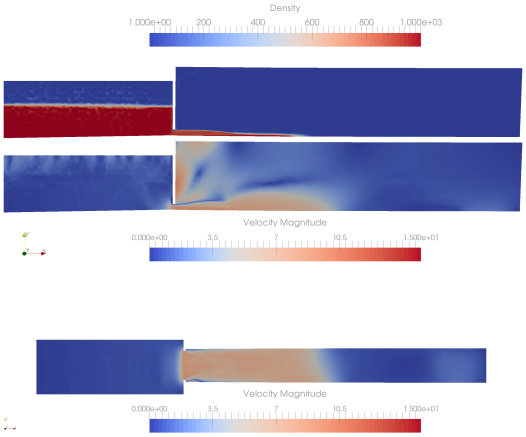

(b) Density and velocity x-y and x-z slice T_D=5s, H=6m, t=5s.

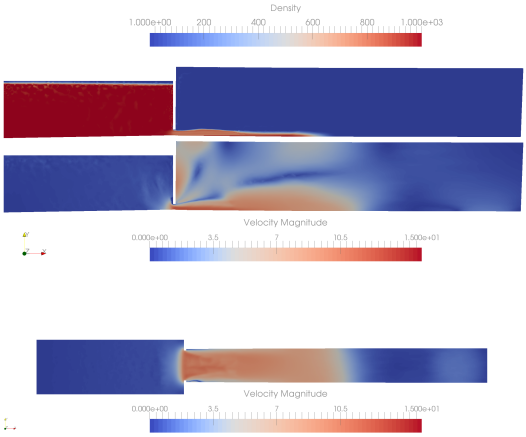

(e) Density and velocity x-y and x-z slice T_D=5s, H=10m, t=5s.

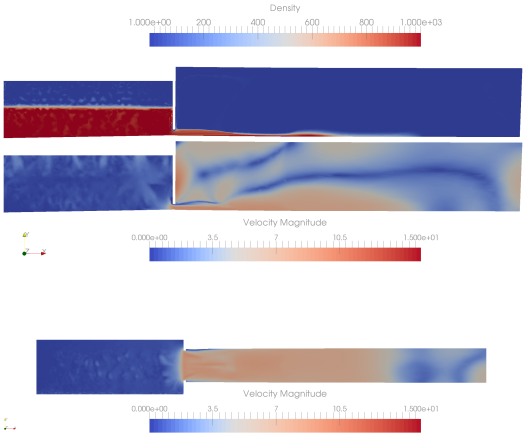

(c) Density and velocity x-y and x-z slice T_D=10s, H=6m, t=10s.

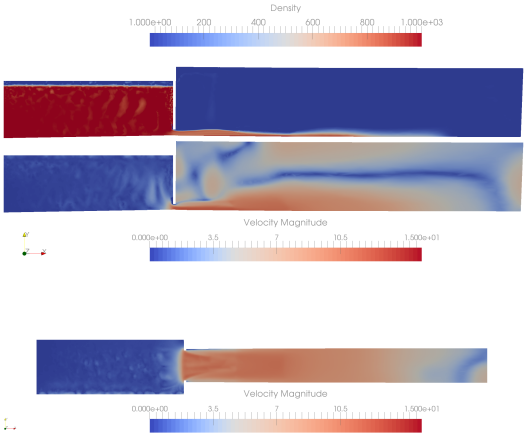

(f) Density and velocity x-y and x-z slice T_D=10s, H=10m, t=10s.

Figure 6: Density and velocity x-y and x-z at different heights with different door opening times.

In this section we plot slice plots of the density (showing the evolution of the water surface), the velocity, 3D plots of the isovolume of the density (showing the evolution of the water surface). Additionally we plot the flow rate through the door over time, and the average velocity in the door section and in the first 10m section of the tunnel.

Figure 6 shows the density and velocity at different times and height settings. As we can see in figure 6 (b) and (e), the turbulent mixing is slightly higher for figure 6 (e); and the velocity at the bottom of the tunnel is also higher in both cases (T_D={5s and 10s}) for H=10m.

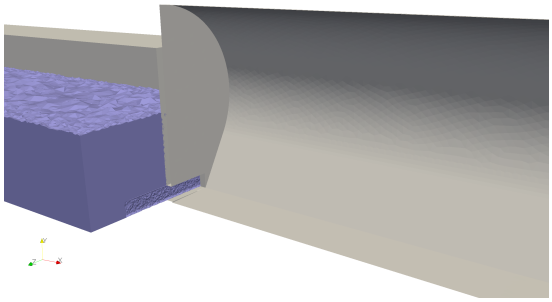

(a) Water isovolume T_D={5s,10s}, H=6m, t=0s

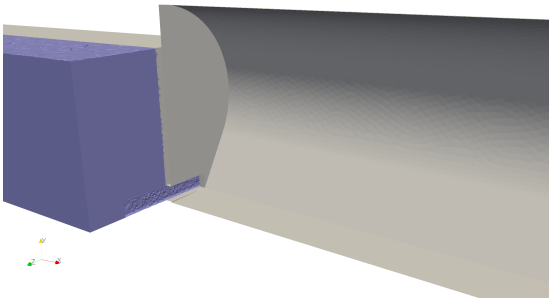

(d) Water isovolume T_D={5s,10s}, H=10m, t=0s

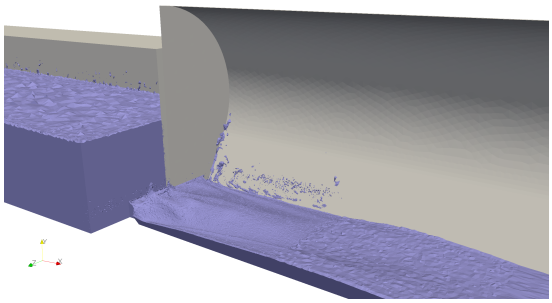

(b) Water isovolume T_D=5s, H=6m, t=5s

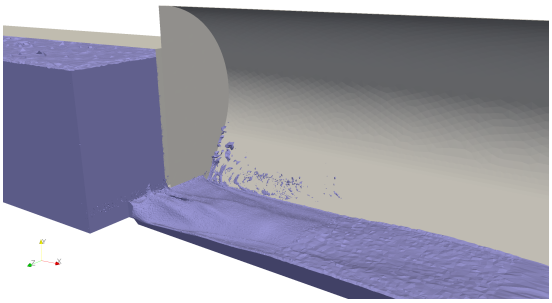

(e) Water isovolume T_D=5s, H=10m, t=5s

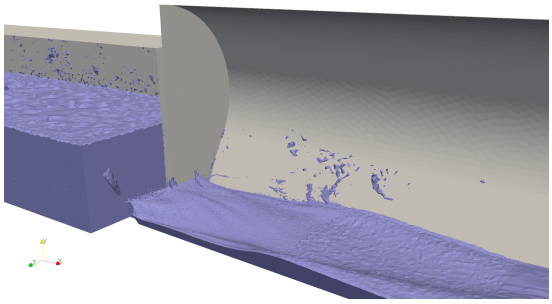

(c) Water isovolume T_D=10s, H=6m, t=10s

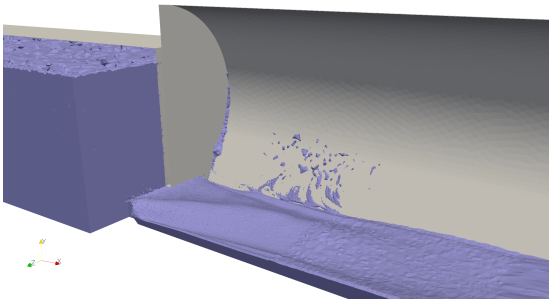

(f) Water isovolume T_D=10s, H=10m, t=10s

Figure 7: Water isovolume at different heights with different door opening times.

Water isovolume in the simulation can be seen in figure 7, where we can see water splashes closer to the door as the gate opens; it is due to pressure difference between tank and tunnel [29] and variable density model which is mentioned in section 3.1. Figure 8 shows the flow rate through the gate. As we can see here, the gate opening time and water height do have a

influence over the water flow rate through the opening gate.

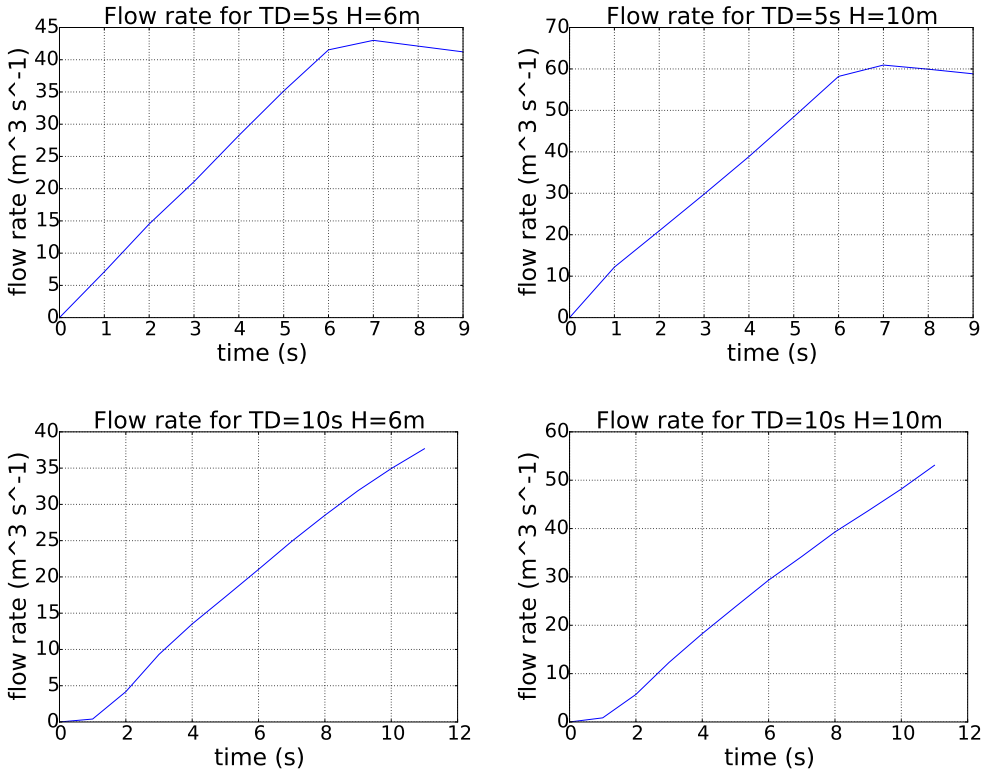

Figure 8: "Spending" flow rate through the door.

Figure 9 shows the average velocity at the door section. It is clear that the velocity is higher at the door section for H=10m compared to H=6m (for the same opening time T_D=5s).

The average velocity at the downstream side of the tunnel is plotted in figure 10. It shows that for T_D=5s and H=6m, the velocity increases gradually up to $6\,\mathrm{m\,s^{-1}}$ until $t = 4s$, after that the velocity goes down. On the other hand, for T_D=5s and H=10m, the velocity is higher, up to ca. $8\,\mathrm{m\,s^{-1}}$. This behaviour is similar to the case of T_D=10s. Thus we can conclude that the water height influences the average velocity at the bottom of the tunnel.

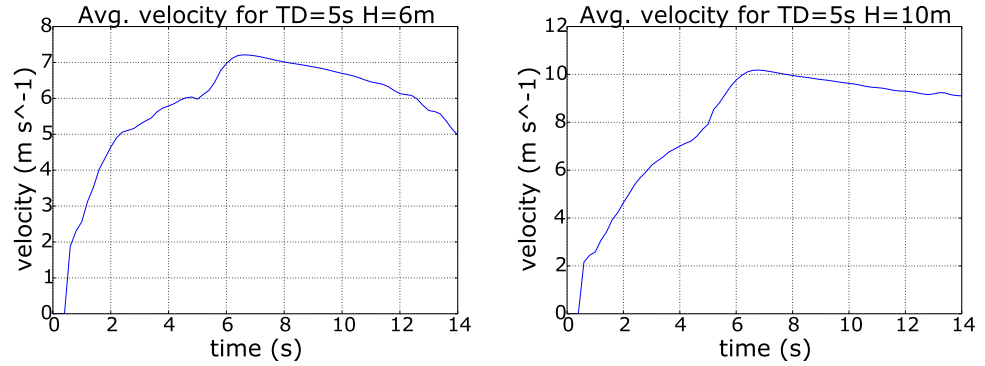

Figure 9: Average x-velocity in the door section.

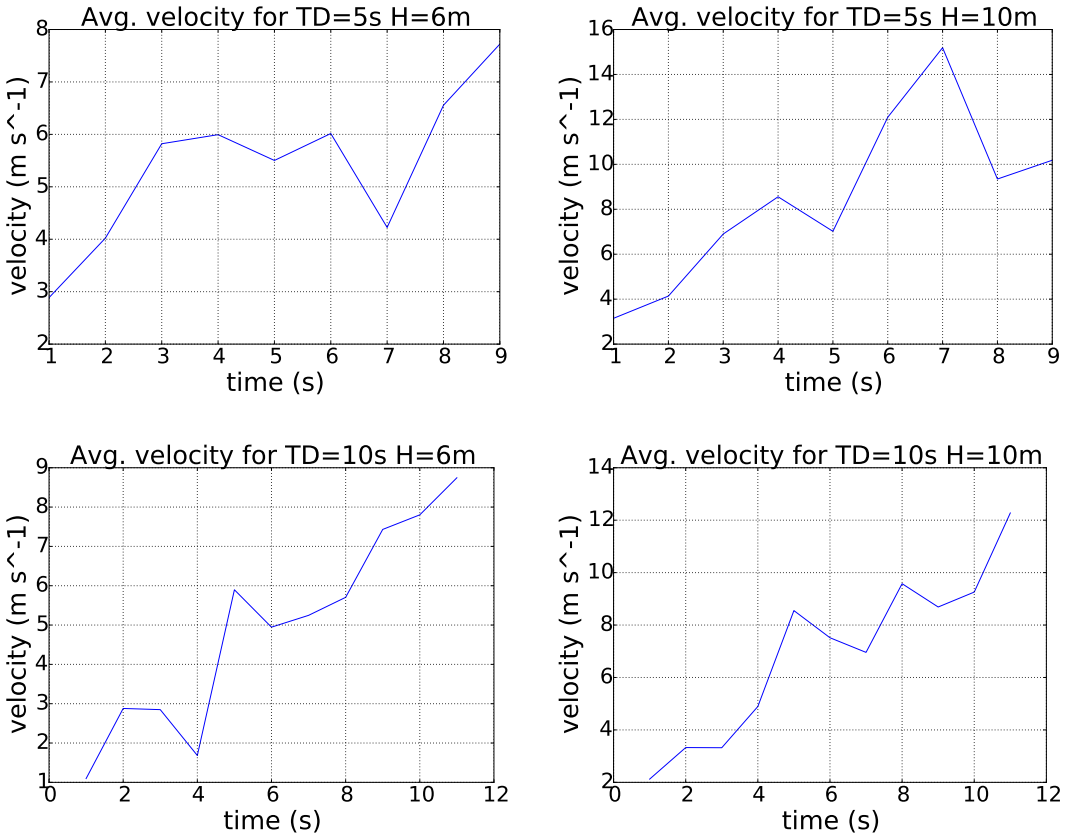

Figure 10: Average flushing x-velocity in the first 10m-section of the tunnel.

6 CONCLUSIONS

In this paper we provide computational results for Direct FEM simulations of the primitive 3D variable-density incompressible Navier-Stokes equations. We investigate the MARIN marine engineering benchmark and a storm drain system.

The simulation results for the MARIN benchmark qualitatively capture the evolution of the pressure signals in the sensors. The discrepancies are quantitatively of approximately similar magnitudes as the state of the art published in the literature, e.g. in [30, 28].

For the storm drain problem, the density and velocity fields have a 3D structure, a triangular jet shape, at the exit of the door. The door opening time does not appear to have a large influence on the structure or magnitude of the velocity. The water height in the tank has a significant influence on the magnitude of the velocity in the flushing section at the beginning of the tunnel.

In future work we would like to study the mesh sensitivity of the method and implement a robust adaptive method, similar to what we have developed for constant density turbulent flow, to enable adaptive error control.

REFERENCES

[1] J Hoffman, J Jansson, RV de Abreu, NC Degirmenci, Niclas Jansson, Kaspar Mller, Murtazo Nazarov, JHiromi Sphler, Unicorn: Parallel adaptive finite element simulation of tur-

bulent flow and fluid-structure interaction for deforming domains and complex geometry. *Computers & Fluids*, 2013.

[2] J Hoffman, J Jansson, N Jansson, FEniCS-HPC: Automated predictive high-performance finite element computing with applications in aerodynamics, PPAM 2015. *Lecture Notes in Computer Science*, 2015.

[3] Jonkman, Sebastiaan N. Global perspectives on loss of human life caused by floods , Springer, 2005.

[4] The International Disaster Database. *http://www.emdat.be/country_profile/index.html*.

[5] Füssel, Hans-Martin and Jol, André and others. *Climate change, impacts and vulnerability in Europe 2012 an indicator-based report*, Luxembourg: Publications Office of the European Union, 2012.

[6] Ezcurra, A and Areitio, J and Herrero, I. Relationships between cloud-to-ground lightning and surface rainfall during 1992–1996 in the Spanish Basque Country area. *Atmospheric research*, Elsevier, 2002.

[7] Johan Hoffman, Johan Jansson, Niclas Jansson, and Rodrigo Vilela De Abreu. To- wards a parameter-free method for high reynolds number turbulent flow simulation based on adaptive finite element approximation. *Computer Methods in Applied Mechanics and Engineering*, 288(0):60-74, 2015. Error Estimation and Adaptivity for Nonlinear and Time-Dependent Problems.

[8] Johan Hoffman, Johan Jansson, and Claes Johnson. New theory of flight. *Journal of Mathematical Fluid Mechanics*, 2015.

[9] Johan Hoffman and Niclas Jansson. *A computational study of turbulent flow separation for a circular cylinder using skin friction boundary conditions*. Ercoftac, series Vol.16, Springer, 2010.

[10] Johan Hoffman and Claes Johnson. *Resolution of dalemberts paradox. J. Math. Fluid Mech.*, Published Online First at www.springerlink.com: 10 December 2008.

[11] Rodrigo Vilela de Abreu, Niclas Jansson, and Johan Hoffman. Adaptive computation of aeroacoustic sources for a rudimentary landing gear. *Int. J. Numer. Meth. Fluids*, 74(6):406-421, 2014.

[12] Johan Hoffman and Claes Johnson. *Computational Turbulent Incompressible Flow: Applied Mathematics Body and Soul Vol 4*. Springer-Verlag Publishing, 2006.

[13] Johan Hoffman and Claes Johnson. *Computational Turbulent Incompressible Flow, volume 4 of Applied Mathematics: Body and Soul*. Springer, 2007.

[14] U. Schumann. Subgrid-scale model for finite difference simulation of turbulent flows in plane channels and annuli. *J. Comput. Phys.*, 18:376-404, 1975.

[15] Johan Hoffman. Computation of mean drag for bluff body problems using adaptive DNS/LES. *SIAM J. Sci. Comput.*, 27(1):184-207, 2005.

[16] Johan Hoffman. Adaptive simulation of the turbulent flow past a sphere. *J. Fluid Mech*., 568:77-88, 2006.

[17] Johan Hoffman. Efficient computation of mean drag for the subcritical flow past a circular cylinder using general galerkin g2. Int. *J. Numer. Meth. Fluids*, 59(11):1241-1258, 2009.

[18] Johan Hoffman and Claes Johnson. A new approach to computational turbulence modeling. *Comput. Methods Appl. Mech. Engrg*., 195:2865-2880, 2006.

[19] Johan Hoffman, Johan Jansson, Rodrigo Vilela de Abreu, Niyazi Cem Degirmenci, Niclas Jansson, Kaspar Mller, Murtazo Nazarov, and Jeannette Hiromi Sphler. Unicorn: Parallel adaptive finite element simulation of turbulent flow and fluid- structure interaction for deforming domains and complex geometry. *Computers and Fluids*, 2012.

[20] Johan Hoffman, Johan Jansson, Cem Degirmenci, Niclas Jansson, and Murtazo Nazarov. Unicorn: a Unified Continuum Mechanics Solver, chapter 18. Springer, 2012.

[21] Niclas Jansson, Johan Hoffman, and Johan Jansson. Framework for Massively Parallel Adaptive Finite Element Computational Fluid Dynamics on Tetrahedral Meshes. *SIAM J. Sci. Comput*., 34(1):C24-C41, 2012.

[22] Robert C. Kirby. *FIAT: Numerical Construction of Finite Element Basis Functions*, chapter 13. Springer, 2012.

[23] Johan Hoffman, Johan Jansson, Niclas Jansson, C. Johnson, and Rodrigo V. de Abreu. Turbulent flow and fluid-structure interaction. In *Automated Solutions of Differential Equations by the Finite Element Method*. Springer, 2011.

[24] Johan Hoffman, Johan Jansson, Niclas Jansson, and Murtazo Nazarov. Unicorn: A unified continuum mechanics solver. In *Automated Solutions of Differential Equations by the Finite Element Method*. Springer, 2011.

[25] FEniCS. Fenics project. *http://www.fenicsproject.org*, 2003.

[26] Anders Logg, Kent-Andre Mardal, Garth N. Wells, et al. *Automated Solution of Differential Equations by the Finite Element Method*. Springer, 2012.

[27] J. Hoffman, J. Jansson, and M. Stckli. Unified continuum modeling of fluid-structure interaction. *Mathematical Models and Methods in Applied Sciences*, 2011.

[28] K.M.T. Kleefsman, G. Fekken, A.E.P. Veldman, B. Iwanowski and B. Buchner: A Volume-of-Fluid based simulation method for wave impact problems. *J. Comp. Phys*, 206, (2005), 363-393.

[29] Xu, Lei and Zhang, Wendy W and Nagel, Sidney R. Drop splashing on a dry smooth surface. *Physical review letters*, APS, 94, 2005.

[30] Kees, C. E., Akkerman, I., Farthing, M. W., Bazilevs, Y. (2011). A conservative level set method suitable for variable-order approximations and unstructured meshes. *Journal of Computational Physics*, 230(12), 4536-4558.